Non-Binary LDPC Code Design for the Poisson PPM Channel

Balázs Matuz, *Member, IEEE*, Enrico Paolini, *Member, IEEE*, Flavio Zabini, *Member, IEEE*, and Gianluigi Liva, *Senior Member, IEEE*

***Abstract*— This paper investigates the design of non-binary protograph low-density parity-check codes for the Poisson channel with m-ary pulse position modulation. The field order over which the code is constructed is matched to the pulse position modulation order yielding a coded modulation scheme. The optimization of the low-density parity-check code structure is performed via protograph density evolution on a surrogate m-ary erasure channel. The surrogate design is illustrated to be not only accurate, but also *robust* for a range of practical values of channel background noise and various modulation orders. As a result the proposed codes show excellent performance over the Poisson channel with pulse position modulation outperforming competing schemes. As a side-product of this paper, finite-length benchmarks on the block error probability are provided, together with a union bound to characterize the code performance in the error floor region.**

***Index Terms*— Channel capacity, channel coding, low-density parity-check codes, photon counting, poisson channel, pulse position modulation.**

I. Introduction

THE Poisson channel has often been exploited as a suitable model for direct detection (photon counting) optical deep space links [1]–[4]. For such links, usually the link budget dictates the use of power efficient modulation schemes, such as on-off keying (OOK) with a non-uniform input distribution [5]. A popular alternative to OOK is m-ary pulse position modulation (PPM) which allows a simple mapping between code symbols and modulation symbols. It turns out to be a nearly optimum solution with a negligible loss compared to OOK when the PPM order is properly chosen [6]. The capacity of the Poisson channel with PPM is known in the literature [5] and has been widely used as a performance reference. On the contrary, finite-length benchmarks for the Poisson PPM channel were mostly neglected in the literature. Yet, they are of great interest, particularly to give insights on the performance of short- and moderate-length codes. Finite-length bounds for standard communication channels include for instance Gallager-like bounds, union bounds (UBs), sphere-packing bounds, and various others [7]–[12]. Recently, benchmarks based on Strassen's normal approximation [13]–[15] raised increasing attention. They make use of a characteristic channel parameter named *dispersion* which captures the second order statistics of information density. They turn out to be a good estimate of the block error probability (BLEP) also for short blocks.

Early works on channel coding for the Poisson channel with PPM focused on Reed-Solomon (RS) codes, where the field size was matched to the PPM order [16], as well as on convolutional codes [17]. Hard-decision decoding in the former and short constraint lengths in the latter case penalize the performance of these codes. With the rise of iterative decoding schemes significant gains were achieved in the setting of bit-interleaved coded modulation with iterative decoding (BICM-ID). For instance, the binary low-density parity-check (LDPC) coding scheme proposed in [18] outperforms a classical RS code by more than 3 dB at a bit error rate of 10^{-5} for 64-ary PPM. Hereby, messages are not only exchanged iteratively between the nodes of the LDPC decoder, but also between the PPM demodulator and the decoder as required by BICM-ID. A competing binary scheme, named serially concatenated pulse position modulation (SCPPM) [19] outperforms the binary LDPC scheme of [18] by a few tenths of dB. It consists of a serial concatenation of an outer convolutional code, an inner code composed of an accumulator and a pulse position modulator. This way a turbo code is obtained which is to the best knowledge of the authors the most powerful iterative coding scheme for the Poisson channel with PPM.

This work considers the design of *non-binary* LDPC codes for the Poisson PPM channel. The proposed approach stems from the observation that on the Poisson PPM channel bit-interleaved coded modulation (BICM) shows a significant loss in capacity compared to coded modulation (CM). To reduce this gap it is mandatory to employ iterative message passing between the demodulator and decoder, yielding a BICM-ID scheme. Alternatively, multilevel coding with multistage decoding can attain the CM capacity by carefully selecting the code rates employed at each bit level of the constellation label. For the non-binary LDPC codes in this paper we match the order of the finite field of the code to the PPM order, yielding a CM scheme with one-to-one mapping between the field elements and the modulation symbols. We simulate the performance of non-binary cycle codes [20],

Manuscript received December 20, 2016; revised May 8, 2017; accepted July 16, 2017. Date of publication July 24, 2017; date of current version November 15, 2017. The work of E. Paolini was supported by ESA/ESTEC under Contract no. 4000118331/16/UK/ND. This paper was presented in part at the IEEE International Conference on Communications 2014, Sydney, Australia, and the IEEE International Symposium on Turbo Codes & Iterative Information Processing 2014, Bremen, Germany. The associate editor coordinating the review of this paper and approving it for publication was D. Declercq. *(Corresponding author: Balázs Matuz.)*

B. Matuz and G. Liva are with the Institute of Communications and Navigation, German Aerospace Center, 82234 Weßling, Germany (e-mail: balazs.matuz@dlr.de; gianluigi.liva@dlr.de).

E. Paolini and F. Zabini are with the Department of Electrical, Electronic, and Information Engineering, University of Bologna, 47521 Cesena, Italy (e-mail: e.paolini@unibo.it; flavio.zabini2@unibo.it).

Color versions of one or more of the figures in this paper are available online at http://ieeexplore.ieee.org.

Digital Object Identifier 10.1109/TCOMM.2017.2730868

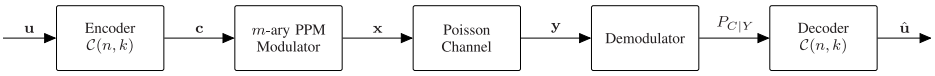

Fig. 1. Block diagram of the communication system. $\mathcal{C}(n,k)$ is constructed over the finite field order of m which is equal to the PPM order m.

since for moderate field orders they show remarkable coding gains on the binary input additive white Gaussian noise (biAWGN) channel with both antipodal and orthogonal modulation schemes [21]–[23]. We illustrate that non-binary cycle codes are sensitive to channel background noise, with large performance degradations at low background radiation levels. We then introduce a surrogate code design which relies on the erasure channel (EC) approximation. The proposed design leads to constructions that not only ensure higher robustness with respect to background noise, but also outperform SCPPM.

As a complement, we compare the performance of the proposed codes with finite-length benchmarks based on the normal approximation. To this end we evaluate its expression for the Poisson PPM channel. As a simpler alternative the normal approximation for a surrogate EC is also provided, underpinning the viability of the surrogate EC approach. Finally, to assess the BLEP in the error floor region, a UB is provided as well.

This work is organized as follows. Section II introduces the problem and notation. Section III gives expressions for capacity results and BLEP benchmarks for the Poisson PPM channel, as well as for a surrogate EC with the same capacity. Section IV addresses the non-binary code design approach. Numerical results for the obtained codes in terms of error rates are provided in Section IV, before concluding the work in Section VI. Further derivations are provided in the Appendix.

II. Preliminaries

Consider the block diagram of a communication system as depicted in Figure 1. Let us denote a linear block code over $\mathbb{F}_q$, the finite field of order q, with block length n [symbols] and information length k [symbols] by $\mathcal{C}(n,k)$. The code rate is $r = k/n$ [symbols/channel use]. Encoding consists of the mapping of a length-k information word $\mathbf{u} = [u_0, \ldots, u_{k-1}]$ onto a length-n codeword $\mathbf{c} = [c_0, \ldots, c_{n-1}]$ as imposed by the code constraints. In this work we focus on the case where $\mathcal{C}(n,k)$ is an LDPC code constructed over $\mathbb{F}_q$. A generic field element is denoted by β_j, $j \in \{0, 1, \ldots, q-1\}$. After encoding we map a codeword $\mathbf{c} = [c_0, \ldots, c_{n-1}]$ of $\mathcal{C}(n,k)$ onto a modulated sequence $\mathbf{x} = [x_0, \ldots, x_{n-1}]$. We are interested in m-ary PPM where the modulation order is matched to the field order, i.e., $m = q$. Each PPM symbol $x_i = [x_i[0], \ldots, x_i[m-1]]$ spans over m time slots, out of which exactly one slot is pulsed while the remaining $m-1$ slots are blank. A PPM symbol for which the jth slot is pulsed is denoted by P_j. The resulting channel input alphabet $\mathcal{X}$ is m-ary with $\mathcal{X} = \{\mathsf{P}_0, \ldots, \mathsf{P}_{m-1}\}$. By convention the modulator performs the bijective mapping $\beta_j \to \mathsf{P}_j$.

We assume transmission over a free-space optical channel with direct detection at the receiver and denote the vector of received symbols by $\mathbf{y} = [y_0, \ldots, y_{n-1}]$. Each received symbol y_i can be subdivided into m time slots yielding $y_i = [y_i[0], \ldots, y_i[m-1]]$, where $y_i[t]$ is the number of received photons in the tth time slot of symbol i. For ease of presentation, whenever possible we drop the index i. Throughout the paper we denote random variables (RVs) by capital letters and the corresponding realizations by small letters. To give an example, $Y[t]$ is the RV corresponding to $y[t]$. Considering a generic time slot t the channel transition probabilities may be well modeled as a memoryless, time-invariant Poisson process with [2]

$$p_1(y[t]) \coloneqq \Pr\{Y[t] = y[t] | X = \mathsf{P}_t\} = \frac{(n_s + n_b)^{y[t]}}{y[t]!} e^{-n_s - n_b} \tag{1a}$$

$$p_0(y[t]) \coloneqq \Pr\{Y[t] = y[t] | X = \mathsf{P}_l\} = \frac{{n_b}^{y[t]}}{y[t]!} e^{-n_b}, \quad t \neq l. \tag{1b}$$

In (1a) and (1b), n_s denotes the average number of received signal photons per pulsed slot and n_b the average number of received noise photons per slot.

At the demodulator we are interested in computing $P_{C|Y}(c|y)$ for all possible values β_j of C. Having a one-to-one mapping between code symbols and modulation symbols, as well as no prior information on the code symbols, we can write $P_{C|Y}(c|y) \propto P_{Y|X}(y|x)$. Moreover, we have

$$\begin{aligned} P_{Y|X}(y|\mathsf{P}_l) &= p_1(y[l]) \prod_{t=0, t\neq l}^{m-1} p_0(y[t]) \\ &= \left(\frac{n_s}{n_b} + 1\right)^{y[l]} e^{-n_s} \prod_{t=0}^{m-1} p_0(y[t]) \\ &\propto \left(\frac{n_s}{n_b} + 1\right)^{y[l]}. \end{aligned} \tag{2}$$

Equation (2) allows computing $P_{C|Y}(c|y)$ which is forwarded to a non-binary LDPC decoder as channel information.

Remark 1: In the setting where $m = q$ the demodulator directly provides symbol wise probabilities to the decoder. No marginalization at the demodulator is performed, unlike for instance for a BICM scheme where bit wise probabilities are computed. Therefore, no loss in information occurs and no iterative exchange of information between decoder and demodulator is necessary.

III. Performance Bounds and Benchmarks

A. Poisson Channel Capacity

For the Poisson channel with m-ary PPM the channel capacity is given by [5]

$$\mathsf{C}_{\mathsf{PPM}} = \log_2 m - \mathbb{E}_{Y|X=\mathsf{P}_0}\left\{\log_2\left(\sum_{t=0}^{m-1} \frac{\Lambda(Y[t])}{\Lambda(Y[0])}\right)\right\} \quad \text{[bits/channel use]} \tag{3}$$

where we have defined the likelihood ratio

$$\Lambda(Y[t]) \coloneqq \frac{p_1(Y[t])}{p_0(Y[t])} = \left(\frac{n_s}{n_b} + 1\right)^{Y[t]} e^{-n_s}.$$

In (3) capacity is expressed in bits per channel use. A channel use corresponds to m time slots. Thus, dividing the result in (3) by m we obtain channel capacity expressed in bits per slot which will be useful in the sequel.

Let us denote a capacity achieving input distribution by $P_X^\star(x)$. For the m-ary Poisson PPM channel we have that a uniform distribution achieves capacity, i.e., $P_X^\star(x) = 1/m$, $\forall x \in \mathcal{X}$ [5]. Further, in Appendix we prove the following lemma.

Lemma 1: For the m-ary Poisson PPM channel with $\mathrm{C_{PPM}} > 0$ *the only capacity achieving input distribution is the uniform distribution.*

Consider now the Poisson channel with OOK. In each time slot either a pulse is transmitted if the corresponding bit at the modulator input is one, or the time slot is left blank if the corresponding bit is a zero. The probability of transmitting a one is denoted by $1/\Delta$. The channel capacity of the Poisson channel with OOK has been studied, e.g., in [5] and is given by

$$\mathrm{C_{OOK}} = \max_{\Delta \geq 1} \Bigg\{ \log_2 \Delta - \frac{1}{\Delta} \mathbb{E}_Y \left\{ \log_2 \left[1 + (\Delta - 1)/\Lambda(Y) \right] \right\} - \frac{\Delta - 1}{\Delta} \mathbb{E}_Y \left\{ \log_2 \left[(\Delta - 1) + \Lambda(Y) \right] \right\} \Bigg\} \quad \text{[bits/slot]} \tag{4}$$

where we dropped the slot index t. Observe that in (4) channel capacity, thus the maximum achievable rate depends on Δ. As a result, as opposed to PPM the mapping of information symbols to OOK modulated symbols such that a certain probability of a pulsed slot $1/\Delta$ is achieved needs to be carefully addressed.

Let γ be the average number of received signal photons per slot. Then, $\gamma = n_s/m$ in case of m-ary PPM and $\gamma = n_s/\Delta$ in case of OOK. The Poisson channel capacity versus γ [dB] $= 10 \log_{10} \gamma$ assuming $n_b = 1$ is illustrated in Figure 2 for both m-ary PPM and OOK. For completeness also the BICM capacity of the Poisson PPM channel for different modulation orders is depicted. Note that once γ is given, e.g. as a result of link budget calculations, it is possible to select the PPM order, such that the loss compared to OOK becomes minor.[1] However, when BICM is considered, there is a notable gap compared to the OOK and PPM capacity curves. In case of 128-ary PPM for instance, we have a gap of approximately 1.1 dB for $\gamma = -14.5$ dB. To overcome this gap the authors in [18] and [19] proposed a BICM-ID scheme, while we rely on a CM scheme.

[1]We point out that for a fixed γ, thus fixed average power, an increase of the PPM order implies an increase of the peak power. Also in the case of OOK lowering the spectral efficiency turns in an increase of the peak power. In the sequel, we will assume no peak power constraints.

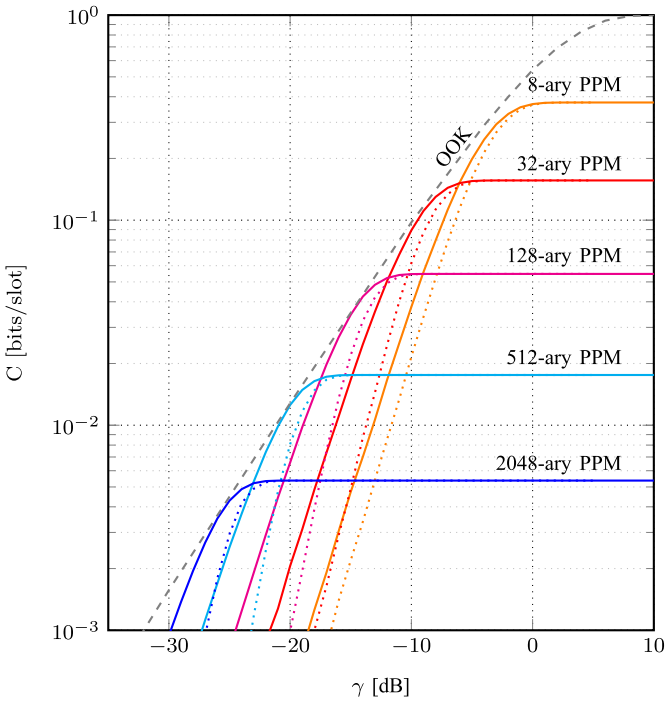

Fig. 2. Solid: capacity of Poisson channel with m-ary PPM vs. γ [dB] for some selected m and $n_b = 1$. Dotted: BICM capacity of Poisson channel with m-ary PPM for $n_b = 1$. Dashed: capacity of the Poisson channel with OOK for $n_b = 1$.

B. Normal Approximation for the Poisson PPM Channel

Let us denote the information density by

$$i(X;Y) \coloneqq \log_2 \frac{P_{X,Y}(x,y)}{P_X(x) P_Y(y)}. \tag{5}$$

Assuming $P_X = P_X^\star$, the channel capacity can be conveniently expressed as

$$\mathrm{C} = \mathbb{E}_{X,Y} \{ i(X;Y) \}$$

while the dispersion of the channel V is defined as the variance of the information density, i.e.,

$$\mathrm{V} \coloneqq \mathrm{Var}\{ i(X;Y) \}. \tag{6}$$

Note that in case there are multiple capacity achieving input distributions, the expression for V may vary depending on the choice of $P_X^\star(x)$. For the Poisson PPM channel we circumvent this issue by making use of Lemma 1 (stating that $P_X^\star(x)$ is unique).

Channel dispersion together with channel capacity yields a simple finite-length benchmark providing an approximate estimate of the BLEP of the best code with parameters (n, k). The result, known as normal approximation is given by [13]

$$P_e \approx Q\left(\left[\mathrm{C} - r \log_2 m \right] \sqrt{\frac{n}{\mathrm{V}}} \right).$$

The expression for the normal approximation was further tightened in [15] by deriving a correction term that plays a role at short block lengths. Here, the correction term is omitted.

The dispersion of the Poisson PPM channel is then given by

$$\begin{aligned} \mathrm{V}_{\mathsf{PPM}} &= \mathbb{E}_{Y|X=\mathsf{P}_0}\left\{\log_2^2\left(\sum_{t=0}^{m-1}\frac{\Lambda\left(Y[t]\right)}{\Lambda\left(Y[0]\right)}\right)\right\} \\ &\quad - \left[\mathbb{E}_{Y|X=\mathsf{P}_0}\left\{\log_2\left(\sum_{t=0}^{m-1}\frac{\Lambda\left(Y[t]\right)}{\Lambda\left(Y[0]\right)}\right)\right\}\right]^2 \\ &= \mathbb{E}_{Y|X=\mathsf{P}_0}\left\{\log_2^2\left(\sum_{t=0}^{m-1}\frac{\Lambda\left(Y[t]\right)}{\Lambda\left(Y[0]\right)}\right)\right\} \\ &\quad - [\log_2\ m - \mathrm{C}_{\mathsf{PPM}}]^2 \quad [\text{bits}^2/\text{channel use}^2] \quad (7) \end{aligned}$$

where we made use of Equations (6), (5), and (3). The expression in (7) can be evaluated numerically via Monte Carlo simulations.

C. Surrogate Erasure Channel Capacity

In absence of background noise, i.e., for $n_b = 0$, the Poisson PPM channel is shot noise dominated and turns into an m-ary EC with erasure probability [16], [17]

$$\epsilon = e^{-n_s}$$

where the capacity of the m-ary EC is known to be

$$\mathrm{C}_{\mathsf{EC}} = (1-\epsilon)\log_2\ m \quad [\text{bits/channel use}].$$

In the sequel we will illustrate that the m-ary EC channel also proves to be a good approximation of the m-ary Poisson PPM channel for small, non-zero values of background noise, typical for deep-space links. More precisely, instead of an m-ary Poisson PPM channel, we will rely on an m-ary EC as a surrogate whose capacity is equivalent to that of the Poisson PPM channel.

Definition 1 (Surrogate m-ary EC): Consider a Poisson channel with m-ary PPM and channel parameters $\gamma = n_s/m$ and n_b. Denote its capacity by $\mathrm{C}_{n_b}(\gamma)$ [bits/channel use].[2] *Then, the corresponding surrogate EC is an m-ary EC with erasure probability*

$$\epsilon = 1 - \frac{\mathrm{C}_{n_b}(\gamma)}{\log_2 m}. \quad (8)$$

D. Normal Approximation for the Surrogate Erasure Channel

Equation (8) allows computing the normal approximation for the surrogate m-ary EC. Observe that the capacity and dispersion for the m-ary EC are given by

$$\begin{aligned} \mathrm{C}_{\mathsf{EC}} &= (1-\epsilon)\log_2\ m \quad [\text{bits/channel use}] \\ \mathrm{V}_{\mathsf{EC}} &= \epsilon\ (1-\epsilon)\log_2^2 m \quad [\text{bits}^2/\text{channel use}^2] \end{aligned}$$

where a channel use corresponds to the transmission of an m-ary symbol, thus of $\log_2\ m$ bits. We obtain

$$P_e \approx Q\left(\frac{\mathrm{C}_{\mathsf{EC}} - r\log_2 m}{\sqrt{\mathrm{V}_{\mathsf{EC}}/n}}\right) = Q\left(\frac{n(1-r)-n\epsilon}{\sqrt{n\epsilon(1-\epsilon)}}\right).$$

Choosing ϵ as in (8) yields the normal approximation for the surrogate m-ary EC.

[2]We rewrite $\mathrm{C}_{\mathsf{PPM}}$ as $\mathrm{C}_{n_b}(\gamma)$ to emphasize the dependency from n_b and γ.

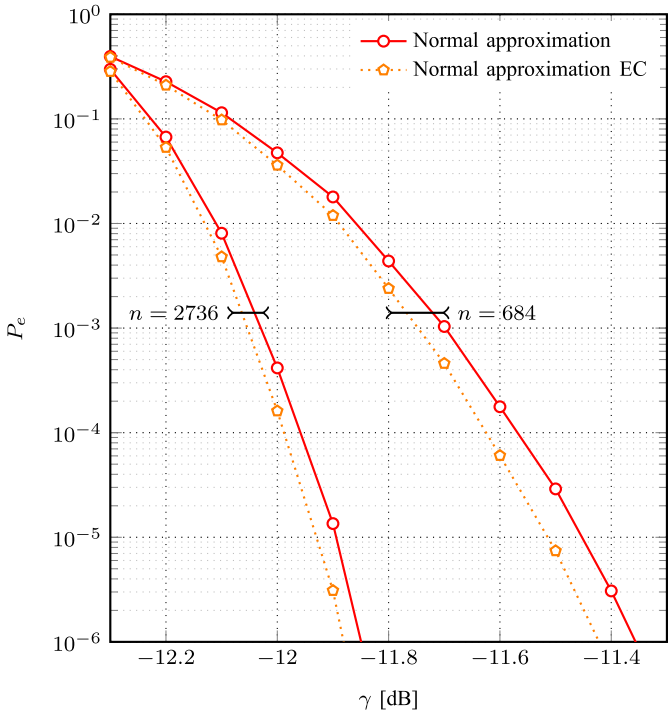

Fig. 3. Normal approximation for the PPM Poisson channel and the surrogate m-ary EC with $m = 16$, $n_b = 0.02$, $n = \{684, 2736\}$, and $r = 0.5$.

Figure 3 depicts the BLEP versus γ [dB] obtained by the normal approximation for the Poisson PPM channel and the surrogate EC. We consider 16-ary PPM with block lengths $n \in \{684, 2736\}$, $r = 1/2$, and $n_b = 0.02$. For both block lengths, the benchmarks lie close to each other, confirming the validity of the surrogate EC for the current setting. In Section V the accuracy of the surrogate EC will be illustrated also for higher values of background noise.

E. Union Bound on the BLEP of a Linear Code

Consider a linear block code $\mathcal{C}(n,k)$ over $\mathbb{F}_q$ under maximum-likelihood (ML) decoding on the Poisson PPM channel. Assume that a generic code symbol is mapped onto a PPM symbol by the bijective mapping $\mathsf{f}: \mathbb{F}_q \to \mathcal{X}$. Then, the probability of decoding error can be expressed by

$$\begin{aligned} P_B &= P_{B|\mathbf{c}_0} \\ &\le \sum_{\mathbf{c}\in\mathcal{C}\setminus\{\mathbf{c}_0\}} \Pr\left\{P_{\mathbf{Y}|\mathbf{X}}(\mathbf{Y}|\mathsf{f}(\mathbf{c})) \ge P_{\mathbf{Y}|\mathbf{X}}(\mathbf{Y}|\mathsf{f}(\mathbf{c}_0))|\,\mathbf{C}=\mathbf{c}_0\right\} \quad (9) \end{aligned}$$

where $P_{B|\mathbf{c}_0}$ is the probability of error given that the all-zero codeword $\mathbf{c}_0$ is transmitted with $\mathsf{f}(\mathbf{c}_0) = \mathbf{x}_0 = [\mathsf{P}_0, \mathsf{P}_0, \ldots, \mathsf{P}_0]$. The above equality is due to all codewords being equiprobable and to the block error probability being independent of the transmitted codeword (of a linear code) over a PPM Poisson channel. The inequality follows from using the standard UB. Let $\mathsf{f}(\mathbf{c}) = \mathbf{x} = [\mathsf{P}_{t_0}, \mathsf{P}_{t_1}, \ldots, \mathsf{P}_{t_{n-1}}]$. Due to the PPM Poisson channel being memoryless, the condition $P_{\mathbf{Y}|\mathbf{X}}(\mathbf{Y}|\mathsf{f}(\mathbf{c})) \ge P_{\mathbf{Y}|\mathbf{X}}(\mathbf{Y}|\mathsf{f}(\mathbf{c}_0))$ is equivalent to

$$\prod_{i=0}^{n-1} P_{Y|X}(Y_i|\,\mathsf{P}_{t_i}) \ge \prod_{i=0}^{n-1} P_{Y|X}(Y_i|\,\mathsf{P}_0).$$

Applying the logarithm on both sides and making use of (2) we obtain

$$\sum_{i=0}^{n-1} (Y_i[t_i] - Y_i[0]) \geq 0.$$

Clearly, out of the n terms in the sum only the ones corresponding to $t_i \neq 0$ are different from zero. The number of such nonzero terms is equal to the Hamming weight d of the codeword $\mathbf{c}$. We denote by $I_{\mathbf{c},\mathbf{c}_0} \subset \{0, 1, \ldots, n-1\}$ the set of indices in which $\mathbf{c}$ and $\mathbf{c}_0$ differ. Then, (9) may be recast as

$$P_B \leq \sum_{\mathbf{c} \in C \setminus \{\mathbf{c}_0\}} \Pr\{Z \geq 0 | \, \mathbf{C} = \mathbf{c}_0\} \tag{10}$$

with

$$Z \coloneqq \sum_{i \in I_{\mathbf{c},\mathbf{c}_0}} Y_i[t_i] - \sum_{i \in I_{\mathbf{c},\mathbf{c}_0}} Y_i[0].$$

Further, we have that $\sum_{i \in I_{\mathbf{c},\mathbf{c}_0}} Y_i[t_i]$ and $\sum_{i \in I_{\mathbf{c},\mathbf{c}_0}} Y_i[0]$ are Poisson distributed RVs with mean $n_b d$ and $(n_s + n_b)d$, respectively. Therefore, the RV Z is Skellam distributed [24] and the pairwise error probability is given by

$$\begin{aligned}\mathsf{PEP}(d) &\coloneqq \Pr\{Z \geq 0 | \, \mathbf{C} = \mathbf{c}_0\} \\ &= e^{-d(n_s+2n_b)} \sum_{z=0}^{\infty} \left(\frac{n_s}{n_b} + 1\right)^{-\frac{z}{2}} \mathsf{I}_z\left(2\, d\sqrt{(n_s n_b + n_b^2)}\right)\end{aligned}$$

where $\mathsf{I}_z(\cdot)$ is the modified Bessel function of first kind. Since codewords of Hamming weight d contribute in the same way to the UB, we may re-state (10) as

$$P_B \leq \sum_{d=1}^{n} A_d \mathsf{PEP}(d) \tag{11}$$

where the weight enumerator (WE) A_d denotes the number of codewords of Hamming weight d. The expression above requires the estimation of the code's distance spectrum, or parts of it yielding a truncated union bound (TUB). A practical approach to obtain an estimate on the lower part of the distance spectrum will be detailed in Section V.

IV. Non-Binary LDPC Code Design

The design of LDPC codes for a general channel usually follows a two-stage approach. In a first design step, an ensemble with good iterative decoding threshold is selected [25]. Then, a finite length code is obtained by picking a graph, for example, with good girth properties [26]. For the first step a fast, reliable tool for deriving the ensemble decoding threshold is required, while for binary LDPC codes efficient techniques relying on density evolution [25] or extrinsic information transfer (EXIT) [27] charts are available. The analysis of the asymptotic performance of non-binary LDPC codes is still challenging due to the need of tracking m-dimensional parameter vectors. Monte Carlo EXIT analysis [28] for non-binary LDPC codes is not well suited as an alternative due to its high computational complexity. Another option is a one-dimensional approximation of the bipartite graph messages [29]. In the following we will resort to this approach. Our approximation is enabled by the observation that, at low background noise values the m-ary Poisson PPM channel resembles an m-ary EC.

A. EXIT Analysis for the Surrogate Erasure Channel

Instead of performing the code design directly on an m-ary Poisson PPM channel we rely on the surrogate m-ary EC from Definition 1. In fact, it is well-established that the calculation of decoding thresholds and search of *binary* LDPC code ensembles on a wide range of binary-input memoryless symmetric channels can be carried out reasonably accurately by using instead a simpler binary EC [30]–[33]. We will pursue a structured LDPC code design based on protographs which are preferable to unstructured designs from an implementation point of view. A binary protograph [34] is a bipartite graph with a relatively small number of variable nodes (VNs) and check nodes (CNs). Each node is assigned an own label or type. The protograph serves as a blueprint for a larger LDPC code which may be obtained by expanding the protograph through "copy-and-permute" operations. To this end, the protograph is copied l times and the edges are permuted among the copies. The permutation must however preserve the neighborhoods of the nodes, i.e., if in the protograph a node of type i was connected to a node of type j, any of the l copies of it must be connected to one of the l nodes of type j after the permutation. Non-binary protographs [35] may additionally possess edge labels from $\mathbb{F}_m \setminus \{0\}$. We focus on unconstrained protographs for which the edge labels are assigned only after the final expansion step. Protographs may be conveniently represented by a base matrix $\mathbf{B} = [b_{ij}]$, where b_{ij} gives the number of edges connecting a CN of type i, named C_i to a VN of type j, named V_j.

Protograph EXIT analysis for the binary EC has been introduced in [36]. In the following we restrict the analysis to the case of $m = 2$, since the iterative decoding threshold of an m-ary LDPC code ensemble on an m-ary EC is independent of m. Therefore, we are free in the choice of m for the threshold computation. We enumerate all edges of the protograph and denote by I_{V_j} the set of indices of all edges emanating from V_j and by I_{C_i} the set of indices of all edges emanating from C_i. In the sequel we fix a certain erasure probability ϵ and track the mutual information for each edge of the protograph for a sufficiently large number of iterations and decide whether for the given erasure probability decoding succeeds or not.

For a VN of type j, let us denote the mutual information between the input message on an edge e and the associated codeword symbol by $\mathsf{I}_{\mathrm{AV}}^{(e)}$, the mutual information between the output message on edge e and the associated codeword symbol by $\mathsf{I}_{\mathrm{EV}}^{(e)}$. For the binary EC with erasure probability ϵ we have for $e \in I_{V_j}$

$$\mathsf{I}_{\mathrm{EV}}^{(e)} = 1 - \epsilon \prod_{\ell \in I_{V_j} \setminus \{e\}} (1 - \mathsf{I}_{\mathrm{AV}}^{(\ell)}). \tag{12}$$

Further, for a CN of type i we define the mutual information between the input message on an edge e and the corresponding code symbol as $\mathsf{I}_{\mathrm{AC}}^{(e)}$ and the mutual information between the output message on an edge e and the corresponding code symbol as $\mathsf{I}_{\mathrm{EC}}^{(e)}$. We have for $e \in I_{C_i}$

$$\mathsf{I}_{\mathrm{EC}}^{(e)} = \prod_{\ell \in I_{C_i} \setminus \{e\}} \mathsf{I}_{\mathrm{AC}}^{(\ell)}. \tag{13}$$

Equations (12) and (13) are iteratively applied to track the evolution of mutual information for the edges of the protograph. To this end in (12) we set the a priori information of a generic edge e to $\mathsf{I}_{\mathrm{AV}}^{(e)} = \mathsf{I}_{\mathrm{EC}}^{(e)}$, where $\mathsf{I}_{\mathrm{EC}}^{(e)} = 0$ for the first iteration. After computation of $\mathsf{I}_{\mathrm{EV}}^{(e)}$ for all edges of the protograph, we set $\mathsf{I}_{\mathrm{AC}}^{(e)} = \mathsf{I}_{\mathrm{EV}}^{(e)}$ and evaluate the extrinsic information for outgoing CN edges as in (13). After a sufficiently large number of iterations between VN and CN operations we compute the mutual information between the a posteriori probabilities at V_j and the corresponding code symbol as

$$\mathsf{I}_{\mathrm{APP}}^{(j)} = 1 - \epsilon \prod_{\ell \in I_{V_j}} (1 - \mathsf{I}_{\mathrm{AV}}^{(\ell)}).$$

The largest value of ϵ for which $\mathsf{I}_{\mathrm{APP}}^{(j)} \to 1$ for all j, is the iterative decoding threshold $\epsilon^\star$.

Once $\epsilon^\star$ is available by protograph EXIT analysis for the EC, we obtain an estimate of the iterative decoding threshold on the corresponding Poisson PPM channel from (8) as

$$\gamma_{\mathsf{EC}}^\star = \mathrm{C}_{n_b}^{-1}\left((1-\epsilon^\star)\log_2 m\right). \tag{14}$$

A further discussion follows in Section IV-C.

B. Code Design for the Surrogate Erasure Channel

We define an LDPC code ensemble $\mathcal{E}^n$ as the set of all m-ary LDPC codes of length n obtained from a base matrix $\mathbf{B}$ by expansion. When n tends to infinity we use the shorthand $\mathcal{E}$ for the ensemble. The non-zero coefficients of a code's parity-check matrix in the ensemble are chosen uniformly at random from $\mathbb{F}_m \backslash \{0\}$.[3]

The surrogate design of non-binary protograph-based LDPC codes is performed as follows:

- Seek for an ensemble $\mathcal{E}$ which possesses an iterative decoding threshold close to the Shannon limit. This optimization is performed via differential evolution [37] and is subject to certain constraints. More precisely, we constrain the number of degree one and two VNs, maximum VN degree, and the size of the base matrix.
- The iterative decoding threshold $\epsilon^\star$ of an ensemble is obtained via protograph EXIT analysis for the *binary* EC as described in Section IV-A.
- Once an ensemble $\mathcal{E}$ is found, expand the underlying protograph by copy-and-permute operations. For this we used a variant of the progressive edge growth (PEG) algorithm [26].
- To obtain a non-binary code, edge labels are assigned, in our case randomly with uniform probability from $\mathbb{F}_m \backslash \{0\}$.

Example 1 (Optimized design 1): For the protograph search we put the following constraints: the size of the base matrix is 3×5 *to keep the search space small. For the optimization we allow at maximum three columns of degree-*2 *or degree-*1*, since an excessive number of degree one and two VNs yields good thresholds, but also high error floors. We allow one punctured column, as punctured protographs are known to show excellent performances [38]. The resulting design rate is* $r = 1/2$*. The optimization yields the base matrix*

$$\mathbf{B}_1 = \begin{bmatrix} 2 & 1 & 1 & 1 & 0 \\ 1 & 2 & 1 & 1 & 0 \\ 2 & 0 & 0 & 0 & 1 \end{bmatrix}$$

which in fact describes a specific accumulate-repeat-accumulate (ARA) LDPC code ensemble [39] assuming that the VN corresponding to first column is punctured. We denote the corresponding ensemble of m*-ary LDPC codes by* $\mathcal{E}_{\mathbf{B}_1}$*. It has an iterative decoding threshold on an* m*-ary EC of* $\epsilon^\star = 0.478$*, independent of* m*.*

Example 2 (Optimized design 2 from [40]): To further improve the decoding threshold we consider bigger protographs. In fact, optimized protographs for the EC were presented in [40]. The protographs in [40] describe Raptor-like, i.e., rate-compatible LDPC code ensembles. We recap a 9×17 *protograph, the first VN being punctured yielding a design rate* $r = 1/2$*. We have*

$$\mathbf{B}_2 = \begin{bmatrix} 3 & 2 & 1 & 1 & 1 & 1 & 1 & 1 & 0 & 0 & 1 & 0 & 0 & 0 & 0 & 0 & 0 \\ 1 & 1 & 2 & 2 & 2 & 2 & 2 & 2 & 2 & 1 & 1 & 0 & 0 & 0 & 0 & 0 & 0 \\ 2 & 0 & 0 & 0 & 0 & 0 & 0 & 0 & 1 & 2 & 0 & 0 & 0 & 0 & 0 & 0 & 0 \\ 2 & 1 & 1 & 1 & 0 & 0 & 0 & 0 & 0 & 0 & 0 & 1 & 0 & 0 & 0 & 0 & 0 \\ 1 & 0 & 1 & 1 & 1 & 0 & 0 & 0 & 1 & 1 & 0 & 0 & 1 & 0 & 0 & 0 & 0 \\ 2 & 1 & 1 & 0 & 0 & 1 & 0 & 0 & 0 & 0 & 0 & 0 & 0 & 1 & 0 & 0 & 0 \\ 2 & 0 & 0 & 1 & 0 & 0 & 1 & 0 & 0 & 1 & 0 & 0 & 0 & 0 & 1 & 0 & 0 \\ 1 & 0 & 0 & 1 & 0 & 0 & 0 & 1 & 0 & 1 & 0 & 0 & 0 & 0 & 0 & 1 & 0 \\ 2 & 1 & 0 & 0 & 1 & 0 & 0 & 0 & 0 & 0 & 0 & 0 & 0 & 0 & 0 & 0 & 1 \end{bmatrix}.$$

The corresponding ensemble is denoted by $\mathcal{E}_{\mathbf{B}_2}$ *with iterative decoding threshold* $\epsilon^\star = 0.487$*.*

C. On the Accuracy of Surrogate Channels

We discuss the accuracy of the surrogate EC approximation. To this end, we estimate the iterative decoding thresholds of some dedicated ensembles on the Poisson PPM channel via Monte Carlo density evolution [28] and denote the threshold by $\gamma_{\mathsf{MC}}^\star$. This technique is computationally expensive and thus not well suited for the protograph search step of the code design, but appropriate to obtain good threshold estimates for single ensembles. A comparison with $\gamma_{\mathsf{EC}}^\star$ obtained from (14) gives insights on the accuracy of the surrogate EC approximation.

Monte Carlo density evolution emulates the non-binary decoder behavior on an infinitely large graph. Assume a given set of channel parameters n_s and n_b. In every iteration a new set of S channel samples is generated for each VN of type j, V_j. Then, for each V_j, S channel messages (in our case m-ary probability mass functions (PMFs)) are computed and processed with a priori messages from the neighboring CNs. Note that for each V_j the VN operator has to be invoked $d_{v,j}S$ times, where $d_{v,j}$ denotes the degree of V_j. At the first iteration no a priori information is available. Each V_j produces S messages on each of its $d_{v,j}$ edges. Next, messages on same edge types are interleaved among each other randomly to emulate the VN and CN connections in the protograph ensemble.

[3]In addition, $\mathcal{E}$ might also be used to describe *unstructured* m-ary LDPC code ensembles with underlying edge oriented degree distribution pair $\lambda(\mathrm{x})$ and $\rho(\mathrm{x})$. Unstructured ensembles from the literature will be considered later for sake of comparison.

Then, each message, i.e., each m-dimensional PMF is permuted. The permutation is owing to the non-binary coefficients in the respective parity-check equation (refer e.g. to [35]). The coefficients are randomly chosen from $\mathbb{F}_m \backslash \{0\}$. At each CN of type i, C_i the CN operator is invoked $d_{c,j}S$ times, where $d_{c,j}$ denotes the the degree of C_i. The result are S messages on each outgoing edge. Again a permutation of each m-ary PMF takes place as imposed by a random field element from $\mathbb{F}_m \backslash \{0\}$. Then, random interleaving of the messages on same edge types is performed as previously. As a result the first iteration of decoding is completed and at each V_j S a priori messages are available per edge. The process described above is iterated for a sufficient number of times. Then, a hard-decision on S a posteriori messages at each V_j is made. If decoding succeeds n_s is decreased else increased. The smallest value of n_s which allows successful decoding yields $\gamma^\star_{\mathsf{MC}}$.

As a further term of comparison, iterative decoding thresholds using a different approximation have been computed. In particular, we adopted a surrogate Gaussian channel introduced in [29] for the EXIT analysis of non-binary coded modulation. We indicate the obtained iterative decoding thresholds as $\gamma^\star_{\mathsf{GC}}$.

Note that all three techniques above yield approximations on the iterative decoding thresholds. In general, we assume Monte Carlo density evolution to be the most accurate one, but also the one with the highest computational burden. The surrogate EC, as well as the surrogate Gaussian channel are strong simplifications. Yet, as discussed in the previous sections, there is evidence that the surrogate EC is a reasonable choice.

Beyond the previously introduced protograph ensembles, we recap some unstructured ensembles from the literature in order to check the accuracy of the surrogate EC approximation for a wider set of ensembles. More specifically, we consider

a) a regular $(3, 6)$ ensemble $\mathcal{E}_{(3,6)}$.
b) a regular $(4, 8)$ ensemble $\mathcal{E}_{(4,8)}$.
c) an irregular ensemble $\mathcal{E}_{\mathsf{IRR}}$ from [41] with edge oriented degree distribution pair $\lambda(\mathrm{x}) = 0.3333\mathrm{x} + 0.6667\mathrm{x}^3$ and $\rho(\mathrm{x}) = \mathrm{x}^5$, where $\lambda(\mathrm{x})$ and $\rho(\mathrm{x})$ are defined as in [41].

Iterative decoding thresholds on the 64-ary PPM Poisson channel in terms of $\gamma^\star$ [dB] for various ensembles are provided in Table I for different background noise levels. The range was chosen to cover low, moderate and high background noise levels for optical deep space links. In the same table, the corresponding Shannon limit is given as well.

First, we compare $\gamma^\star_{\mathsf{MC}}$ with $\gamma^\star_{\mathsf{EC}}$ to get an insight on the quality of the surrogate EC assumption. Observe that for all ensembles the thresholds lie close to each other. To give an example, for the irregular ensemble $\mathcal{E}_{\mathsf{IRR}}$ the difference between both thresholds is within 0.1 dB for the whole range of n_b. For $\mathcal{E}_{\mathbf{B}_1}$ the difference in the threshold predictions is virtually zero for $n_b = 0.002$ while we have a difference of 0.2 dB for $n_b = 2$. In fact we observe that the EC approximation gets more and more optimistic for increasing n_b. Still, the surrogate m-ary EC mimics the m-ary Poisson PPM channel behavior well for the values of background noise and ensembles in Table I.

TABLE I
ITERATIVE DECODING THRESHOLDS IN TERMS OF $\gamma^\star$ [dB] FOR DIFFERENT ENSEMBLES OVER $\mathbb{F}_{64}$ FOR VARIOUS n_b

		Background noise n_b			
		0.002	0.02	0.2	2
$\mathcal{E}_{\mathbf{B}_1}$	$\gamma^\star_{\mathsf{MC}}$	−18.87	−17.54	−15.19	−11.71
	$\gamma^\star_{\mathsf{EC}}$	−18.86	−17.56	−15.32	−11.90
	$\gamma^\star_{\mathsf{GC}}$	−18.26	−17.04	−14.88	−11.58
$\mathcal{E}_{\mathbf{B}_2}$	$\gamma^\star_{\mathsf{MC}}$	−18.93	−17.50	−15.07	−11.59
	$\gamma^\star_{\mathsf{EC}}$	−18.96	−17.66	−15.40	−11.98
	$\gamma^\star_{\mathsf{GC}}$	−17.96	−16.76	−14.66	−11.40
$\mathcal{E}_{(3,6)}$	$\gamma^\star_{\mathsf{MC}}$	−18.41	−17.10	−14.93	−11.58
	$\gamma^\star_{\mathsf{EC}}$	−18.30	−17.08	−14.92	−11.60
	$\gamma^\star_{\mathsf{GC}}$	−18.08	−16.88	−14.74	−11.46
$\mathcal{E}_{(4,8)}$	$\gamma^\star_{\mathsf{MC}}$	−17.87	−16.64	−14.47	−11.19
	$\gamma^\star_{\mathsf{EC}}$	−17.78	−16.64	−14.56	−11.30
	$\gamma^\star_{\mathsf{GC}}$	−17.34	−16.22	−14.22	−11.04
$\mathcal{E}_{\mathsf{IRR}}$	$\gamma^\star_{\mathsf{MC}}$	−18.62	−17.35	−15.13	−11.71
	$\gamma^\star_{\mathsf{EC}}$	−18.56	−17.32	−15.10	−11.76
	$\gamma^\star_{\mathsf{GC}}$	−18.28	−17.06	−14.90	−11.58
Shannon limit		−19.13	−17.79	−15.51	−12.08

TABLE II
ITERATIVE DECODING THRESHOLDS IN TERMS OF $\gamma^\star$ [dB] FOR $\mathcal{E}_{\mathbf{B}_1}$ FOR VARIOUS MODULATION/FIELD ORDERS m AND DIFFERENT n_b

		Background noise n_b		
m		0.002	0.2	2
16	$\gamma^\star_{\mathsf{MC}}$	−13.10	−9.93	−6.48
	$\gamma^\star_{\mathsf{EC}}$	−13.10	−9.94	−6.56
Shannon limit		−13.30	−10.14	−6.72
64	$\gamma^\star_{\mathsf{MC}}$	−18.87	−15.19	−11.71
	$\gamma^\star_{\mathsf{EC}}$	−18.86	−15.32	−11.90
Shannon limit		−19.13	−15.51	−12.08
256	$\gamma^\star_{\mathsf{MC}}$	−24.46	−20.52	−17.08
	$\gamma^\star_{\mathsf{EC}}$	−24.44	−20.78	−17.36
Shannon limit		−24.72	−20.94	−17.56

Consider now the thresholds for the surrogate Gaussian channel $\gamma^\star_{\mathsf{GC}}$. Notable inaccuracies for low values of n_b can be observed for all the ensembles while for high n_b the surrogate Gaussian channel assumption becomes reasonable. To give an example, for $\mathcal{E}_{\mathbf{B}_1}$ and $n_b = 0.002$ there is a gap to $\gamma^\star_{\mathsf{MC}}$ of approximately 0.6 dB while for $n_b = 2$ this gap is reduced to 0.15 dB. In summary the results in the table indicate that a surrogate Gaussian channel is a good model for high n_b. However, compared to the surrogate EC, it is less robust to different, in particular low values of n_b.

Comparing the threshold $\gamma^\star_{\mathsf{MC}}$ of the optimized protograph ensemble $\mathcal{E}_{\mathbf{B}_1}$ with the Shannon limit in Table I we find that for $n_b = 0.002$ there is a gap of 0.3 dB while for $n_b = 2$ this gap increases to 0.4 dB. Therefore, the code ensemble seems to be a good and robust choice for various n_b. Regarding the second optimized $\mathcal{E}_{\mathbf{B}_2}$ we have a gap to the Shannon limit of 0.2 dB for $n_b = 0.002$, while for $n_b = 2$ a gap of 0.5 dB to the Shannon limit can be observed.

In Table II we present iterative decoding thresholds $\gamma^\star_{\mathsf{MC}}$ and $\gamma^\star_{\mathsf{EC}}$ for the ensemble $\mathcal{E}_{\mathbf{B}_1}$ for different m and n_b. Observe

from the table that EC approximation is reasonably accurate for different modulation orders m and n_b. For increasing m and high n_b one may notice a slightly increasing gap between $\gamma^\star_{\mathsf{EC}}$ and $\gamma^\star_{\mathsf{MC}}$. To give an example for $m = 256$ and $n_b = 2$ we have a gap to $\gamma^\star_{\mathsf{MC}}$ of around 0.28 dB while for $m = 16$ and $n_b = 2$ the gap is only 0.10 dB.

V. Simulation Results

A. Error Rates for Different Background Noise Values

Consider a Poisson channel with 64-ary PPM where the modulation order was chosen in alignment with the requirements for optical deep-space links. Assume background noise levels $n_b \in \{0.002, 0.2, 2\}$. The chosen set covers low, moderate and high levels of background noise for deep-space links. The normal approximation for both Poisson PPM channel and surrogate EC were computed for $n = 1368$ [symbols] and $r = 1/2$. redThe results are provided in Figure 4. Observe that in the considered range of n_b both finite-length benchmarks are close to each other.

Further, a 64-ary LDPC code $\mathcal{C}^{64}_{\mathbf{B}_1}(1368, 684)$ from the ensemble $\mathcal{E}^{1368}_{\mathbf{B}_1}$ was constructed and simulated for the specified values of background noise. Belief propagation decoding with a maximum of 100 iterations was used. The codeword error rate (CER) versus γ [dB] is depicted in Figure 4. Note that the obtained performance is within 0.4 dB from the normal approximation at a CER of 10^{-3} and $n_b = 0.002$. For larger n_b the gap slightly increases owing to the fact that the ensemble choice was done on the surrogate EC. For $n_b = 0.2$, for instance, the gap to the normal approximation is around 0.5 dB. In fact this slight loss can also be observed when comparing the iterative decoding thresholds with the corresponding Shannon limits in Table I. Still, the proposed design turns out to be very robust for the considered range of background noise.

Additionally, a 64-ary cycle code $\mathcal{C}^{64}_{(2,4)}(1368, 684)$ was constructed and simulated. Cycle codes are ultra-sparse regular LDPC codes for which every VN is of degree two. For low n_b in accordance with the iterative decoding thresholds in Table I, there is a large gap in coding gain to the optimized LDPC code. For instance, at a CER of 10^{-3} the gap is around 2.5 dB. For increasing n_b however, this gap is progressively recovered and reduces to around 0.4 dB for $n_b = 2$ at a CER of 10^{-3}. Therefore, the cycle code may turn into a viable option for very large n_b. Still, for the considered background noise levels the cycle codes show visible error floors.

In order to predict the error floor for the codes in Figure 4, we made use of the expression in (11) which requires knowledge of the code's distance spectrum. We estimated the lower part of the distance spectrum, more precisely the first two non-zero summands in (11), yielding a TUB. The estimation was done with help of Monte Carlo CER simulations on the 64-ary EC. To this end, we recorded low-weight erasure patterns that make an ML decoder fail. In a subsequent step we checked whether the erasure pattern coincides with the support of a codeword. For the cycle code we found 1260 codewords of weight 8 and 9135 codewords of weight 10. For protograph LDPC code 15 codewords of weight 54 and 480 codewords

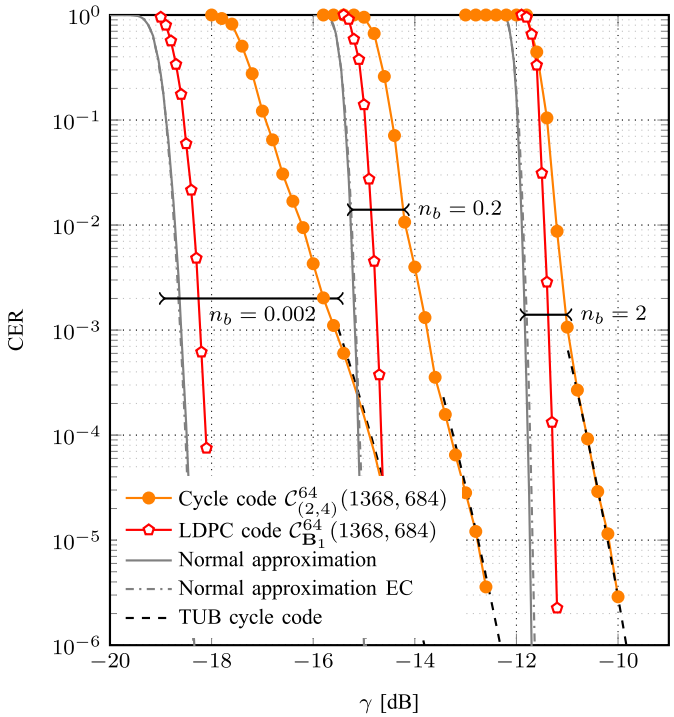

Fig. 4. CER vs. γ [dB] on the 64-ary Poisson PPM channel with $n_b \in \{0.002, 0.2, 2\}$ for an LDPC code $\mathcal{C}_{\mathbf{B}}(1368, 684)$, as well as a cycle code $\mathcal{C}_{(2,4)}(1368, 684)$. As benchmarks the normal approximation its equivalent for the surrogate EC are depicted. TUBs for the cycle codes are also provided.

of weight 55 were found.[4] The resulting truncated UB for the cycle code is depicted in Figure 4. We point out that the UB in (11) is an upper bound BLEP under ML decoding. Due to suboptimal iterative decoding of LDPC codes and truncation, CERs larger than the UB may be obtained. From Figure 4 we observe that the UB predicts the code's error floor performance accurately for the specified values of n_b.

B. Comparison With Serially Concatenated PPM

A performance comparison of a 64-ary LDPC code $\mathcal{C}^{64}_{\mathbf{B}_1}(2520, 1260)$ from the ensemble $\mathcal{E}^{2520}_{\mathbf{B}_1}$ with the SCPPM scheme from [19] on the Poisson channel with 64-ary PPM and $n_b = \{0.0025, 0.2, 2.0\}$ is shown in Figure 5. Currently, SCPPM is amongst the most powerful non-binary iterative coding schemes on the Poisson channel, outperforming binary LDPC codes with BICM-ID [18]. The scheme consists of an outer binary convolutional code which generates 15200 code bits out of 7558 information bits with a nominal rate of $1/2$. After interleaving the code symbols are forwarded to an inner encoder. It consists of a binary accumulator, as well as a PPM mapper (modulator) and outputs in total 2520 encoded 64-ary PPM symbols. For decoding, $\log_2 m$ trellis sections of the inner accumulator are merged and decoded together. This way we have a non-binary inner decoder operating on m-ary symbols. After marginalization of the symbol-wise probabilities and deinterleaving an outer decoding step by means of the Bahl–Cocke–Jelinek–Raviv (BCJR) is done. Inner and outer decoder iteratively exchange messages among

[4] In fact, it is possible that codewords of lower weight exist that were not captured by the Monte Carlo simulations.

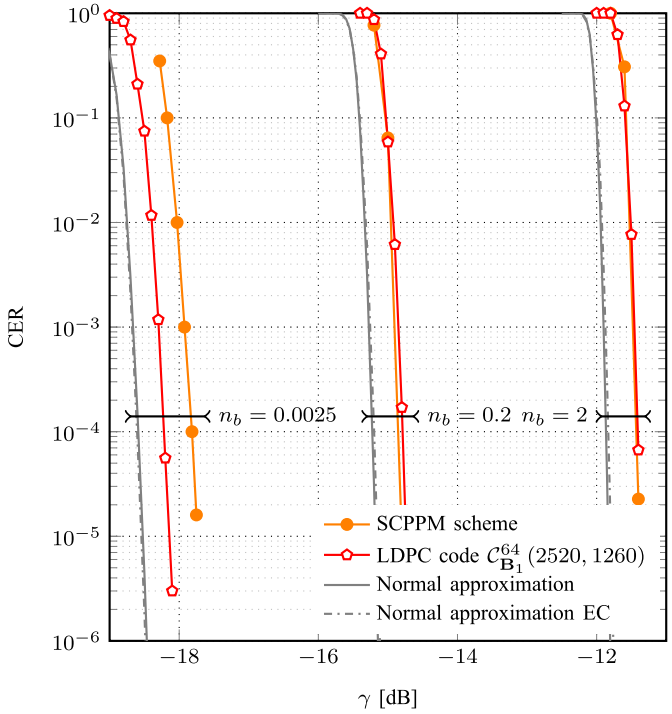

Fig. 5. CER vs. γ [dB] on the 64-ary PPM Poisson channel with $n_b \in \{0.0025, 0.2, 2\}$ for LDPC code $\mathcal{C}^{64}_{\mathbf{B}_1}(2520, 1260)$, as well as for SCPPM scheme with same block and approximately same information length in terms of 64-ary symbols. As benchmarks the normal approximation and its equivalent for the surrogate EC are also depicted.

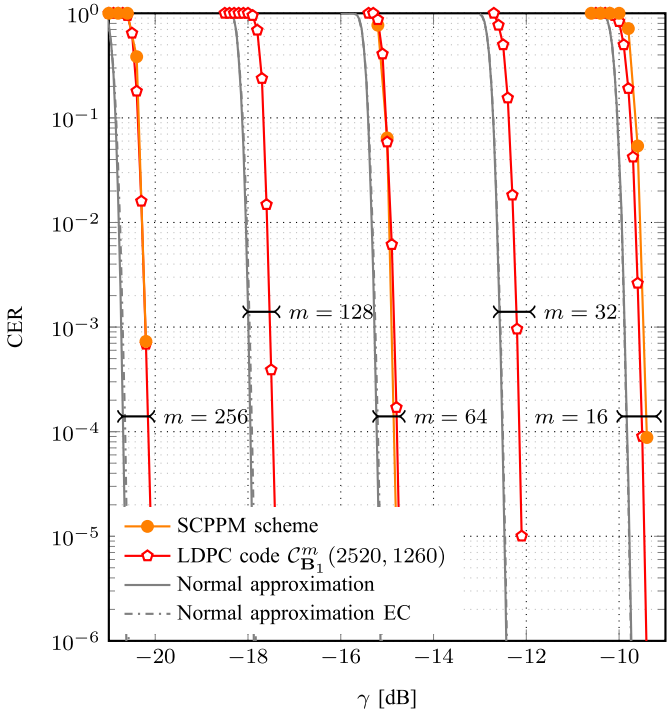

Fig. 6. CER vs. γ [dB] on the m-ary PPM Poisson channel with $n_b = 0.2$ for LDPC codes $\mathcal{C}^{m}_{\mathbf{B}_1}(2520, 1260)$, as well as for SCPPM scheme with same block in terms of 64-ary symbols. As benchmarks the normal approximation and its equivalent for the surrogate EC are also depicted.

each other. This way a powerful serially concatenated turbo-like scheme is obtained.

Figure 5 also depicts the normal approximation for the Poisson PPM channel, as well as for the surrogate EC. Observe that the LDPC code performs within 0.4 dB from the benchmarks at a CER of 10^{-3} which is in alignment with the previous results. Further, the SCPPM scheme shows a gap of approximately 0.4 dB with respect to the LDPC code for $n_b = 0.0025$. For increasing n_b this gap vanishes and for $n_b = 2$ both codes show similar performance. However, unlike the SCPPM scheme the non-binary LDPC code shows nearly a constant gap to the depicted benchmarks, underpinning the robustness of the EC approximation.

Remark 2: The decoding complexity of SCPPM scales similarly to the one of non-binary LDPC codes. The complexity of non-binary LDPC codes is dominated by the $(n-k)$ CN operations. From the literature we have that the decoding complexity per CN scales as $O(m \log_2 m)$ (see e.g. [35]). For SCPPM decoding of the inner non-binary code drives decoding complexity (for sufficiently large m). We found that the critical steps are the computation of the branch metric and the extrinsic information (see also [19]). Consider the branch metric computation. For one trellis section out of k we have $2m$ edges, m of them with distinct edge labels. Thus we need to compute m branch metrics. For the each branch metric symbol-wise priors out of bitwise priors have to be computed in each iteration. Following the log-domain implementation in [19] this requires among others $\log_2 m - 1$ summations. Thus, in total we have that computational complexity scales as $O(m \log_2 m)$. Similar considerations can be made for the computation of the extrinsic information where we have to perform operations on $2m$ edges per trellis section and a marginalization involving $\log_2 m$ bits.

C. Code Performance for Various m

As a complement to Table II we picked and simulated different LDPC codes from the ensemble $\mathcal{E}^{2520}_{\mathbf{B}_1}$ for various m. More precisely, for all simulations we fixed $n = 2520$, $R = 1/2$ and $n_b = 0.2$. We chose the PPM order (field order) from $m = \{16, 32, 64, 128, 256\}$. As benchmarks we computed the normal approximation and its equivalent for the surrogate EC. One may observe from Figure 6 a slight increase of the gap between the normal approximation and the code performance for large m as predicted by the iterative decoding threshold results in Table II. For instance, for $m = 16$ and $m = 256$ the gap merely increases by less than 0.2 dB. Thus, the proposed non-binary codes are not only robust with respect to different background noise values, but also to different modulation orders. To complement Figure 6 also the performance of the SCPPM scheme is depicted for the same block length and same nominal code rate. Observe that for the selected background noise level the performance of SCPPM and the LDPC code is very similar for different modulation orders.

D. LDPC Codes in the Long Block Regime

We designed two long 64-ary LDPC codes $\mathcal{C}^{64}_{\mathbf{B}_1}(10560, 5280)$ and $\mathcal{C}^{64}_{\mathbf{B}_2}(10560, 5280)$ from the respective ensembles in Examples 1 and 2. CER performances

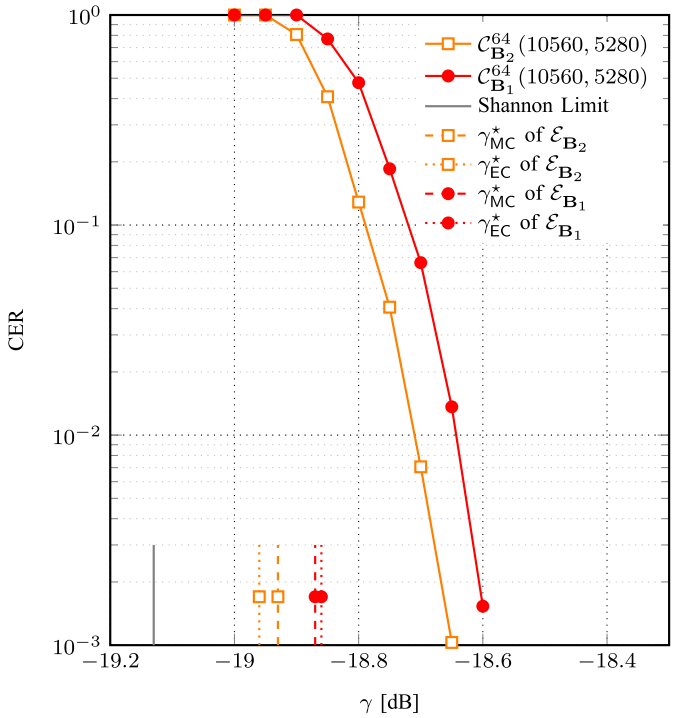

Fig. 7. CER vs. γ [dB] on the 64-ary PPM Poisson channel with $n_b = 0.002$ for LDPC codes $\mathcal{C}^{64}_{\mathbf{B}_1}(10560, 5280)$ and $\mathcal{C}^{64}_{\mathbf{B}_2}(10560, 5280)$. As a benchmark the Shannon limit is depicted, as well as iterative decoding thresholds $\gamma^\star_{\mathsf{MC}}$ and $\gamma^\star_{\mathsf{EC}}$.

versus γ [dB] are depicted in Figure 7 for background noise $n_b = 0.002$. Additionally, the iterative decoding thresholds $\gamma^\star_{\mathsf{MC}}$, $\gamma^\star_{\mathsf{EC}}$, and the Shannon limit are indicated by vertical lines. Observe that the estimated iterative decoding thresholds $\gamma^\star_{\mathsf{MC}}$ reflect accurately the region where the CER curves starts decreasing. Likewise, the gaps between the thresholds $\gamma^\star_{\mathsf{MC}}$ of the two code ensembles are reflected in the respective CER curves. We find that code $\mathcal{C}^{64}_{\mathbf{B}_2}(10560, 5280)$ slightly outperforms $\mathcal{C}^{64}_{\mathbf{B}_1}(10560, 5280)$. Note that in both cases $\gamma^\star_{\mathsf{EC}}$ lies close to $\gamma^\star_{\mathsf{MC}}$.

VI. Conclusions

This work investigates the design of non-binary protograph-based LDPC codes for the Poisson channel with m-ary PPM. For the code design we made use of a surrogate EC model. It has been illustrated that the surrogate EC model is an accurate choice for a considerable range of channel background noise values, as well as modulation orders. We found that constructed LDPC codes notably outperform one of the most powerful non-binary iterative decoding schemes for the Poisson PPM channel, namely SCPPM for low values of background noise. For instance, simulation results show a gap of approximately 0.4 dB for $n_b = 0.0025$ and $m = 64$.

As a reference, also finite-length benchmarks for the Poisson PPM channel based on Strassen's converse theorem normal approximation were evaluated. Also a simple, but accurate expression is provided for the normal approximation on the surrogate EC. The proposed LDPC codes were shown to perform within 0.4 dB from the derived benchmarks in the waterfall region for various background noise values and modulation order $m = 64$. For higher and lower modulation orders the gap to the finite length benchmarks nearly stays unchanged. This underpins the robustness of the proposed design.

In summary, non-binary LDPC codes designed on a surrogate EC show excellent performance on the Poisson PPM channel. Similarly to SCPPM, non-binary LDPC codes have the burden of higher decoding complexity compared to their binary competitors. Nevertheless, they are well-suited for photon efficient deep-space links with moderate data rates in the orders of some Mbps. Further investigations might consider the use of simplified decoders.

Appendix
Proof of Lemma 1

It is known that a uniform input distribution $P^\star_X(x) = 1/m$ achieves channel capacity of the m-ary Poisson PPM channel [5]. We argue that it is the only capacity achieving input distribution for $\mathsf{C}_{\mathsf{PPM}} > 0$. We introduce the shorthand W to denote our communication channel with transition probabilities $P_{Y|X}(y|x)$. One may decompose W into (infinitely many) strongly symmetric channels $W^{(0)}, W^{(1)}, \ldots$ as follows. Denote by $y^{(\ell)} = [y^{(\ell)}[0], y^{(\ell)}[1], \ldots, y^{(\ell)}[m-1]]$ a specific channel output value. Let the set of all cyclic shifts of $y^{(\ell)}$ be

$$\mathcal{Y}^{(\ell)} := \left\{ y^{(\ell)}, y^{(\ell)}\mathbf{M}^1, \ldots, y^{(\ell)}\mathbf{M}^{m-1} \right\}$$

where the $m \times m$ matrix $\mathbf{M}$ is given by

$$\mathbf{M} = \begin{bmatrix} 0 & 1 & 0 & \ldots & 0 & 0 \\ 0 & 0 & 1 & \ldots & 0 & 0 \\ \vdots & \vdots & \vdots & \ddots & \vdots & \vdots \\ 0 & 0 & 0 & \ldots & 0 & 1 \\ 1 & 0 & 0 & \ldots & 0 & 0 \end{bmatrix}.$$

Then, the ℓth strongly symmetric channel has input alphabet $\mathcal{X} = \{\mathsf{P}_0, \ldots, \mathsf{P}_{m-1}\}$ and output alphabet $\mathcal{Y}^{(\ell)}$ and transition matrix $\mathbf{P}^{(\ell)} = \left[P^{(\ell)}_{i,j}\right]$, with $P^{(\ell)}_{i,j} = P_{Y|X}(y^{(\ell)}\mathbf{M}^j|\mathsf{P}_i)/Q_\ell$ and $Q_\ell = \sum_{y \in \mathcal{Y}^{(\ell)}} P_{Y|X}(y|\mathsf{P}_i)$. The original channel is hence equivalent to the set of strongly symmetric channels, where each channel $W^{(\ell)}$ is selected with probability Q_ℓ [43]. Now for proving that the $P^\star_X(x) = 1/m$ is the unique capacity achieving input distribution it is sufficient to observe that

a) $P^\star_X(x) = 1/m$ is capacity-achieving for each channel $W^{(i)}$
b) There exists at least one channel $W^{(i)}$ for which $P^\star_X(x) = 1/m$ is the unique capacity-achieving distribution.

We have that a) is a direct consequence of strong symmetry [44], while b) can be shown by means of a simple example. Consider, e.g., the channel $W^{(\ell')}$ with input alphabet $\mathcal{X}$ and output alphabet

$$\mathcal{Y}^{(\ell')} \in \{[1, 0, 0, \ldots, 0], [0, 1, 0, \ldots, 0], [0, 0, 1, \ldots, 0], \ldots, [0, 0, 0, \ldots, 1]\}.$$

The transition matrix $\mathbf{P}^{(\ell')}$ can be easily obtained from (2) and describes an m-ary symmetric channel (m-SC) with error probability $\lambda = 1/(n_s/n_b + m)$. For an m-SC it is known that the uniform input distribution is the only capacity achieving one, given that channel capacity is non-zero.

ACKNOWLEDGMENTS

The authors would like to thank Achraf Kamoun for providing his SCPPM implementation for CER simulations. Further, they are thankful for all the comments by the Associate Editor and the Reviewers who helped to improve the paper.

REFERENCES

[1] A. D. Wyner, "Capacity and error exponent for the direct detection photon channel. I," *IEEE Trans. Inf. Theory*, vol. 34, no. 6, pp. 1449–1461, Nov. 1988.

[2] R. M. Gagliardi and S. Karp, *Optical Communications*. New York, NY, USA: Wiley, 1976.

[3] H. Hemmati, *Optical Modulation and Coding*. New York, NY, USA: Wiley, 2006, pp. 215–299.

[4] A. Lapidoth and S. M. Moser, "On the capacity of the discrete-time poisson channel," *IEEE Trans. Inf. Theory*, vol. 55, no. 1, pp. 303–322, Jan. 2009.

[5] B. Moision and J. Hamkins, "Deep-space optical communications downlink budget: Modulation and coding," Caltech, Pasadena, CA, USA, IPN Prog. Rep. 42–154, Aug. 2003.

[6] R. Lipes, "Pulse-position-modulation coding as near-optimum utilization of photon counting channel with bandwidth and power constraints," Caltech, Pasadena, CA, USA, DSN Prog. Rep. 42–56, Jan. 1980.

[7] C. E. Shannon, "Probability of error for optimal codes in a Gaussian channel," *Bell Syst. Tech. J.*, vol. 38, no. 3, pp. 611–656, 1959.

[8] R. G. Gallager, "A simple derivation of the coding theorem and some applications," *IEEE Trans. Inf. Theory*, vol. 11, no. 1, pp. 3–18, Jan. 1965.

[9] G. Poltyrev, "Bounds on the decoding error probability of binary linear codes via their spectra," *IEEE Trans. Inf. Theory*, vol. 40, no. 4, pp. 1284–1292, Jul. 1994.

[10] A. M. Viterbi and A. J. Viterbi, "Improved union bound on linear codes for the input-binary AWGN channel, with applications to turbo codes," in *Proc. IEEE Int. Symp. Inf. Theory*, Cambridge, MA, USA, Aug. 1998, p. 29.

[11] D. Divsalar, "A simple tight bound on error probability of block codes with application to turbo codes, the telecommunications and mission operations," NASA JPL, Pasadena, CA, USA, TMO Prog. Rep. 42-139, Nov. 1999.

[12] S. Shamai and I. Sason, "Variations on the Gallager bounds, connections, and applications," *IEEE Trans. Inf. Theory*, vol. 48, no. 12, pp. 3029–3051, Dec. 2002.

[13] V. Strassen, "Asymptotische Abschätzungen in Shannons Informationstheorie," in *Proc. Trans. 3rd Prague Conf. Inf. Theory*, Prague, Czech Republic, Jun. 1962, pp. 689–723.

[14] M. Hayashi, "Information spectrum approach to second-order coding rate in channel coding," *IEEE Trans. Inf. Theory*, vol. 55, no. 11, pp. 4947–4966, Nov. 2009.

[15] Y. Polyanskiy, V. Poor, and S. Verdu, "Channel coding rate in the finite blocklength regime," *IEEE Trans. Inf. Theory*, vol. 56, no. 5, pp. 2307–2359, May 2010.

[16] R. McEliece, "Practical codes for photon communication," *IEEE Trans. Inf. Theory*, vol. 27, no. 4, pp. 393–398, Jul. 1981.

[17] J. Massey, "Capacity, cutoff rate, and coding for a direct-detection optical channel," *IEEE Trans. Commun.*, vol. 29, no. 11, pp. 1615–1621, Nov. 1981.

[18] M. F. Barsoum, B. Moision, M. Fitz, D. Divsalar, and J. Hamkins, "EXIT function aided design of iteratively decodable codes for the poisson PPM channel," *IEEE Trans. Commun.*, vol. 58, no. 12, pp. 3573–3582, Dec. 2010.

[19] B. Moision and J. Hamkins, "Coded modulation for the deep-space optical channel: Serially concatenated pulse-position modulation," Caltech, Pasadena, CA, USA, IPN Prog. Rep. 42-161, May 2005.

[20] M. C. Davey and D. MacKay, "Low-density parity check codes over GF(q)," *IEEE Commun. Lett.*, vol. 2, no. 6, pp. 165–167, Jun. 1998.

[21] C. Poulliat, M. Fossorier, and D. Declercq, "Design of regular $(2, d_c)$-LDPC codes over GF(q) using their binary images," *IEEE Trans. Commun.*, vol. 56, no. 10, pp. 1626–1635, Oct. 2008.

[22] G. Liva, E. Paolini, B. Matuz, S. Scalise, and M. Chiani, "Short turbo codes over high order fields," *IEEE Trans. Commun.*, vol. 61, no. 6, pp. 2201–2211, Jun. 2013.

[23] B. Matuz, G. Liva, E. Paolini, M. Chiani, and G. Bauch, "Low-rate nonbinary LDPC codes for coherent and blockwise non-coherent AWGN channels," *IEEE Trans. Commun.*, vol. 61, no. 10, pp. 4096–4107, Oct. 2013.

[24] J. G. Skellam, "The frequency distribution of the difference between two Poisson variates belonging to different populations," *J. Roy. Statist. Soc. A*, vol. 109, no. 3, p. 296, 1946.

[25] T. J. Richardson and R. L. Urbanke, "The capacity of low-density parity-check codes under message-passing decoding," *IEEE Trans. Inf. Theory*, vol. 47, no. 2, pp. 599–618, Feb. 2001.

[26] X.-Y. Hu, E. Eleftheriou, and D. M. Arnold, "Regular and irregular progressive edge-growth tanner graphs," *IEEE Trans. Inf. Theory*, vol. 51, no. 1, pp. 386–398, Jan. 2005.

[27] S. ten Brink, "Convergence behavior of iteratively decoded parallel concatenated codes," *IEEE Trans. Commun.*, vol. 49, no. 10, pp. 1727–1737, Oct. 2001.

[28] D. MacKay, *Information Theory, Inference & Learning Algorithms*. New York, NY, USA: Cambridge Univ. Press, 2002.

[29] A. Bennatan and D. Burshtein, "Design and analysis of nonbinary LDPC codes for arbitrary discrete-memoryless channels," *IEEE Trans. Inf. Theory*, vol. 52, no. 2, pp. 549–583, Feb. 2006.

[30] S.-Y. Chung, "On the construction of some capacity-approaching coding schemes," Ph.D. dissertation, Dept. Elect. Eng. Comput. Sci., Massachusetts Inst. Technol., Cambridge, MA, USA, 2000.

[31] F. Peng, W. E. Ryan, and R. D. Wesel, "Surrogate-channel design of universal LDPC codes," *IEEE Commun. Lett.*, vol. 10, no. 6, pp. 480–482, Jun. 2006.

[32] M. Franceschini, G. Ferrari, and R. Raheli, "Does the performance of LDPC codes depend on the channel?" *IEEE Trans. Commun.*, vol. 54, no. 12, pp. 2129–2132, Dec. 2006.

[33] I. Sason and B. Shuval, "On universal LDPC code ensembles over memoryless symmetric channels," *IEEE Trans. Inf. Theory*, vol. 57, no. 8, pp. 5182–5202, Aug. 2011.

[34] J. Thorpe, "Low-density parity-check (LDPC) codes constructed from protographs," NASA JPL, Pasadena, CA, USA, IPN Prog. Rep. 42-154, Aug. 2003.

[35] L. Costantini, B. Matuz, G. Liva, E. Paolini, and M. Chiani, "Nonbinary protograph low-density parity-check codes for space communications," *Int. J. Satellite Commun. Netw.*, vol. 30, no. 2, pp. 43–51, Mar./Apr. 2012.

[36] G. Liva and M. Chiani, "Protograph LDPC codes design based on EXIT analysis," in *Proc. IEEE Global Telecommun. Conf. (GLOBECOM)*, Washington, DC, USA, Nov. 2007, pp. 3250–3254.

[37] A. Shokrollahi and R. Storn, "Design of efficient erasure codes with differential evolution," in *Differential Evolution: A Practical Approach to Global Optimization*. Springer, 2005, pp. 413–427.

[38] D. Divsalar, S. Dolinar, C. R. Jones, and K. Andrews, "Capacity-approaching protograph codes," *IEEE J. Sel. Areas Commun.*, vol. 27, no. 6, pp. 876–888, Aug. 2009.

[39] A. Abbasfar, K. Yao, and D. Divsalar, "Accumulate-repeat-accumulate codes," in *Proc. IEEE Global Telecommun. Conf.*, Dallas, TX, USA, Nov. 2004, pp. 509–513.

[40] K. Vakilinia, D. Divsalar, and R. D. Wesel, "Protograph-based Raptor-like LDPC codes for the binary erasure channel," in *Proc. IEEE Inf. Theory Appl. Workshop*, San Diego, CA, USA, Feb. 2015, pp. 240–246.

[41] B. Matuz, G. Toscano, G. Liva, E. Paolini, and M. Chiani, "A robust pulse position coded modulation scheme for the Poisson channel," in *Proc. IEEE Int. Conf. Commun.*, Sydney, NSW, Australia, Jun. 2014, pp. 2118–2123.

[42] *High Photon Efficiency Optical Communications Coding & Modulation, White Book, Draft 2, Consultative Committee for Space Data Systems (CCSDS) Draft for Recommended Standard XXX.0-B-0.2*, document CCSDS XXX.0-B-0.2, Sep. 2015.

[43] I. Land and J. Huber, "Information combining," *Found. Trends Commun. Inf. Theory*, vol. 3, no. 3, pp. 227–330, Nov. 2006.

[44] R. Gallager, *Information Theory and Reliable Communication*. New York, NY, USA: Wiley, 1968.

Balázs Matuz (M'14) was born in Budapest, Hungary, in 1982. He received the Diploma degree in electrical engineering and information technology from the Technische Universität München (TUM) in 2007 and the Ph.D. degree from the Technische Universität Hamburg-Harburg in 2013. Since 2007, he has been an Associate Researcher with the German Aerospace Center (DLR), Oberpfaffenhofen, where he mainly involved in novel forward error correcting schemes for satellite and space communication systems. In 2012, he spent a sabbatical term at the University of Bologna, as a recipient of the DLR Research Semester Grant. Since 2014, he has been a Co-Lecturer for channel codes for iterative decoding with the Institute for Communications Engineering, TUM. His main research interests include error control coding, particularly low-density parity-check codes, signal processing, and channel modeling. He has been active in the DVB-SH standardization and in the CCSDS standardization of error correcting codes. He received the Exemplary Reviewer Award for the IEEE Communications Letters. He serves the IEEE as a reviewer for transactions, journals, and conferences, and as a technical program committee member.

Enrico Paolini (M'07) received the Dr.-Ing. (*summa cum laude*) degree in telecommunications engineering and the Ph.D. degree in electrical engineering from the University of Bologna, Italy, in 2003 and 2007, respectively. While working toward the Ph.D. degree, he was a Visiting Research Scholar with the Department of Electrical Engineering, University of Hawai'i at Manoa, Honolulu, HI. He was a Visiting Senior Scientist with the Institute of Communications and Navigation, German Aerospace Center, in 2012 and 2014, under DLR-DAAD fellowships. He joined the Department of Electrical, Electronic, and Information Engineering "Guglielmo Marconi", University of Bologna, as an Assistant Professor in 2010, and was promoted to Associate Professor in 2015. He is a frequent Visitor with the Institute of Communications and Navigation, German Aerospace Center. He has contributed to several projects funded by the European Space Agency (ESA), including NEXCODE (next generation uplink coding techniques), HELIOS (highly reliable links during solar conjunctions), SCAT (C-band transceiver for small satellites). His research interests include error correcting codes, iterative decoding algorithms, random access protocols with successive interference cancellation, detection, and estimation algorithms. In the field of error correcting codes, he has been involved in several scientific activities with ESA since 2004. He served on the organizing committee (as the co-chair) of the IEEE ICC'14, the IEEE ICC'15, and the IEEE ICC'16 Workshop on Massive Uncoordinated Access Protocols, and (as a treasurer) of the 2011 IEEE International Conference on Ultra-Wideband. He served on the Technical Program Committee at several IEEE international conferences, including ICC, Globecom, and ISIT. Since 2015, he has been an Associate Editor of the Communication Theory for the IEEE TRANSACTIONS ON COMMUNICATIONS. He is a past Associate Editor (2012–2015) of the IEEE COMMUNICATIONS LETTERS.

Flavio Zabini (M'13) received the Laurea (*summa cum laude*) degree in telecommunications engineering and the Ph.D. degree in electronic engineering and computer science from the University of Bologna, Italy, in 2004 and 2010, respectively. He was with IEIITBo of CNR. In 2004, he has developed his master's thesis at the University of California at San Diego. In 2008, he was a Visiting Student with DoCoMo Eurolabs, Munich, Germany. From 2013 to 2014, he was a Post-Doctoral Fellow with the German Aerospace Center, Oberpfaffenhofen, Germany. He is currently a Researcher with the University of Bologna. His current research interests include channel coding for free space optical links, echo cancellation for on-channel repeaters, random sampling techniques applied to sensor networks, and performance-fairness tradeoff in communication systems.

Gianluigi Liva (M'08-SM'14) was born in Spilimbergo, Italy, in 1977. He received the M.S. and Ph.D. degrees in electrical engineering from the University of Bologna, Italy, in 2002 and 2006, respectively. Since 2003, he has been investigating channel codes for high data rate Consultative Committee for Space Data Systems (CCSDS) missions. From 2004 to 2005, he was researching at the University of Arizona, Tucson, where he was designing low-complexity error correcting codes for space communications. Since 2006, he has been with the Institute of Communications and Navigation, German Aerospace Center (DLR), where he currently leads the Information Transmission Group. In 2010, he has been appointed lecturer for channel coding at the Institute for Communications Engineering (LNT), Technische Universität München (TUM). In 2012 and 2013, he was lecturing for channel coding at the Nanjing University of Science and Technology, China. Since 2014, he has been a Lecturer for channel codes with iterative decoding with LNT, TUM. He received the Italian National Scientific Habilitation (ASN) as a Full Professor in telecommunication engineering in 2017. His main research interests include satellite communications, random access techniques, and error control coding. He is/has been active in the DVB-SH, DVB-RCS and DVB-S2 standardization groups, and in the standardization of error correcting codes for deep-space communications within the CCSDS. He received the 2007 IST Mobile & Wireless Communication Summit Best Paper Award. He has been the Co-Chair of the First DLR Workshop on Random Access and Coding (2013), the 2014 Sino-German Workshop Bridging Theory and Practice in Wireless Communications and Networking in Shenzhen, China, the IEEE ICC 2014 Workshop on Massive Uncoordinated Access Protocols in Sydney, Australia, and the 2015 Munich Workshop on Coding and Modulation.